ATLAS NOTE

ATLAS-CONF-2011-140

September 24, 2011

Measurement of $t\bar{t}$ production in the all-hadronic channel in 1.02 fb^{-1} of pp collisions at $\sqrt{s} = 7$ TeV with the ATLAS detector

The ATLAS Collaboration

Abstract

We present a measurement of the $t\bar{t}$ production cross-section in the all-hadronic channel. The analysis is performed using 1.02 fb^{-1} of pp collisions produced at the LHC with a centre-of-mass energy of $\sqrt{s} = 7$ TeV and recorded with the ATLAS detector. After selecting events passing a multi-jet trigger and kinematic requirements, we require events to have two reconstructed jets identified as b-jets. After preselection, an *Event Mixing* method is used to model the kinematics of a higher jet-multiplicity multi-jet sample from a lower jet-multiplicity one, depleted in signal events. The total $t\bar{t}$ cross-section is then extracted using a binned likelihood fit of the χ^2 from a kinematic fit assuming the $t\bar{t}$ event hypothesis, and measured to be $\sigma_{t\bar{t}} = 167 \pm 18$ (stat.) ± 78 (syst.) ± 6 (lum.) pb, consistent with the Standard Model prediction. As a cross-check of this analysis, an alternative one using a method exploiting b-tagging information and the centrality of the events, the *ABCD* method, is also discussed.

ATLAS-CONF-2011-140
05/10/2011

1 Introduction

The study of the top quark, the most massive particle observed so far in the Standard Model (SM), is one of the highest priorities of the ATLAS physics program. In particular, the measurement of the top quark pair ($t\bar{t}$) production cross-section (for pp collisions with a center-of-mass energy of $\sqrt{s}$ = 7 TeV this is predicted to be $\sigma^{t\bar{t}}_{\rm SM} = 164^{+11}_{-16}$ pb [1, 2, 3, 4] assuming a top quark mass of 172.5 GeV) is important because it tests QCD perturbative calculations and because $t\bar{t}$ events constitute a major background to several new physics scenarios.

In the SM, the top quark decays into a W boson and a b-quark with almost 100% probability. The W boson subsequently decays into either a quark-antiquark pair or a lepton and neutrino. We present in this note a measurement of $t\bar{t}$ production in the all-hadronic final state where both W bosons decay hadronically, characterized by a nominal six-jet topology. This channel has the advantage of a large branching ratio (46% [5]) but it suffers from a large QCD multi-jet background.

The results presented in this document are based on pp collisions at a centre-of-mass energy of $\sqrt{s}$ = 7 TeV produced at the Large Hadron Collider (LHC) and recorded with the ATLAS detector [6] in 2011 for an integrated luminosity of 1.02 fb^{-1}. This work follows the analysis which was based on 2010 data and an integrated luminosity of 36 pb^{-1}, which resulted in an observed (expected) upper limit on the $t\bar{t}$ total production cross-section, assuming the SM branching ratios to the all-hadronic state, of 261 (314) pb at 95% confidence level [7]. This work is complementary to other ATLAS $t\bar{t}$ cross-section measurements performed in the single lepton and dilepton channels [8, 9, 10].

This note is structured as follows. A description of the ATLAS detector along with the data and Monte Carlo simulation samples is given in Section 2. To isolate the $t\bar{t}$ signal, several kinematic and topological characteristics of the signal can be exploited together with b-jet identification requirements based on a secondary-vertex-based algorithm (b-tagging). The reconstructed object definitions and event selections are described in Section 3. After preselection, the Event Mixing algorithm, described in Section 4, is used to reconstruct the mass χ^2 background distribution built on the hypothesis of a $t\bar{t}$ final state and to measure the cross-section as described in Section 5. As cross check of the Event Mixing analysis, the results produced with the ABCD method are described in Section 6. A review of the sources of systematic uncertainties is given in Section 7, and finally the summary can be found in Section 8.

2 Detector, data and simulated samples

The ATLAS detector consists of a set of cylindrical sub-detectors that cover almost fully the solid angle[1] around the interaction point. It is composed of an inner tracking system close to the interaction point and surrounded by a superconducting solenoid, electromagnetic and hadronic calorimeters, and a muon spectrometer with three superconducting air-core toroid magnet systems. A three-level trigger system is used in ATLAS to select interesting events produced in pp collisions. The Level-1 trigger, implemented in hardware, uses a subset of the available detector information to reduce the event rate to no greater than 75 kHz. This trigger is followed by two software-based trigger levels, Level-2 and the Event Filter, used together to reduce the event rate to about 200 Hz.

The data used in this analysis were collected during the 2011 data taking period with pp collisions at $\sqrt{s}$ = 7 TeV. All data used in this analysis were recorded with stable beam conditions with all relevant subsystems fully operational and represent a total integrated luminosity of 1.02 fb^{-1} with an uncertainty of 3.7% [11]. The data sample has been collected with un-prescaled multi-jet triggers, which for most

[1] In the right-handed ATLAS coordinate system, the pseudorapidity η is defined as η = - ln[tan(θ/2)], where the polar angle θ is measured with respect to the LHC beamline. The azimuthal angle ϕ is measured with respect to the x-axis, which points towards the centre of the LHC ring. The z-axis is parallel to the anti-clockwise beam viewed from above. Transverse momentum and energy are defined as $p_{\rm T} = p\,\sin\theta$ and $E_{\rm T} = E\,\sin\theta$, respectively. The distance ΔR is defined as $\Delta R = \sqrt{(\Delta\phi)^2 + (\Delta\eta)^2}$.

of the period correspond to a trigger that requires five jets with $|\eta| < 3.2$ and $E_{\mathrm{T}} > 10$ GeV at Level-1, 25 GeV at Level-2 and 30 GeV at the Event Filter [12]. For our baseline event selection a requirement of at least five offline jets with $E_{\mathrm{T}} > 55$ GeV is used, for this cut the single jet trigger efficiency is 90%, the plateau of 100% is reached only for jets with $E_{\mathrm{T}} > 60$ GeV.
The modelling of $t\bar{t}$ signal and its associated selection efficiency is derived from Monte Carlo (MC). For the MC generation of the $t\bar{t}$ signal, the the MC@NLO v3.41 [13] generator with PDF set CTEQ6.6 [14] was used to tune the selection criteria and build a signal template to fit the data, assuming a top quark mass of 172.5 GeV. The POWHEG [15] generator was used as an alternative to study the systematic uncertainty due to the signal modelling. The generated events were processed through the full ATLAS detector simulation based on GEANT4 [16] followed by the trigger and offline reconstruction. Due to the large uncertainty in the QCD multi-jet cross-section prediction, we employed a data-driven technique described in Section 4 to estimate the background. The cross-check analysis requires the use of a simulated set of standard background processes (W+jets, Z+jets, single top and dibosons) [17].

3 Object definition and event selection

3.1 Jets

Jets are reconstructed with the anti-k_{t} algorithm [18, 19] with a distance parameter $R = 0.4$. The inputs to the jet reconstruction are topological clusters calibrated at the electromagnetic (EM) scale. A jet energy calibration based on a p_{T}- and η-dependent correction derived from MC simulation is applied. If a jet is closer than ΔR=0.2 to an electron identified as discussed below, the jet is removed from consideration to avoid double-counting. Only jets with $p_{\mathrm{T}} > 20$ GeV and $|\eta| < 4.5$ are considered in this analysis. A detailed description of the jet definition can be found in Refs. [20, 21].

3.2 Identification of b-jets

The identification of jets originating from a b-quark is performed using a secondary-vertex-based tagging algorithm, called JetFitter [22]. JetFitter exploits the topology of weak b- and c-hadron decays inside the jet. A Kalman filter is used to find a common line on which the primary vertex and the b- and c-hadron decay vertices lie, as well as their positions on this line, giving an approximated flight path for the b-hadron. With this approach, the b- and c-hadron vertices are not necessarily merged, even when only a single track is attached to each of them. The discrimination between b-, c- and light-jets is based on a likelihood using the masses, momenta, flight-length significances, and track multiplicities of the reconstructed vertices as inputs. To further increase the flavour discrimination power, a second b-tagger (IP3D) [22] is run, that does not attempt to directly reconstruct decay vertices. Instead, this tagger uses the transverse and the longitudinal impact parameter significances of each track within the jet to determine a likelihood that the jet originates from a b-quark. The IP3D and JetFitter tagger results are combined using an artificial neural network to determine a single discriminant variable (JetFitterCombNN) that is used to make tagging decisions. For this analysis we tune this cut to accept b-jets with approximately 60% efficiency on simulated $t\bar{t}$ events. This corresponds to a light jet rejection factor of about 350.

3.3 Leptons and missing transverse energy

The all-hadronic $t\bar{t}$ channel nominally has six jets and does not contain intrinsic missing transverse energy ($E_{\mathrm{T}}^{\mathrm{miss}}$) or isolated leptons in the final state. Therefore, to avoid overlap with other $t\bar{t}$ cross-section measurements and to reduce the background due to events containing W bosons that decay leptonically,

a veto against high-p_{T} isolated leptons and significant $E_{\mathrm{T}}^{\mathrm{miss}}$ is applied. The leptons and $E_{\mathrm{T}}^{\mathrm{miss}}$ used for this veto are defined according to the following criteria:

- Electron candidates are required to pass a standard tight electron selection as defined in Ref. [8], with $p_{\mathrm{T}} > 20$ GeV and $|\eta_{\mathrm{cluster}}| < 2.47$, but excluding the barrel-endcap calorimeter transition region at $1.37 < |\eta| < 1.52$. In order to suppress background from hadrons faking an electron signature, electrons from heavy-flavour decays and photon conversions, an isolation criteria is applied to the selected electrons. The selected electron is required to have little jet activity in the space surrounding its direction ($\Delta R < 0.2$). The energy measured in a cone of $\Delta R < 0.2$ centered around the electron direction is required to be below 3.5 GeV.

- Muons are reconstructed by combining the measurements of the tracks detected in the muon spectrometer with those of the associated track in the inner detector [8]. Good muon candidates are selected by requiring $p_{\mathrm{T}} > 20$ GeV and $|\eta| < 2.5$. An additional isolation requirement is applied to select only muons with both a p_{T} sum of calorimeter clusters and of tracks in a cone with $R = 0.3$ around the muon candidate of less than 4 GeV.

- The missing transverse energy, $E_{\mathrm{T}}^{\mathrm{miss}}$, is an object-based definition calculated from topological clusters calibrated at the EM scale and corrected according to the energy scale of the associated object. Calorimeter clusters not associated to any high p_T object are included at the EM scale and corrections for the muon/electron candidates are applied [20, 21].

3.4 Event selection

Events are selected by first requiring that the trigger signature described in Section 2 is satisfied. A series of kinematic cuts are applied to the events to define the signal region. Events are first required to have:

- no isolated lepton with $p_{\mathrm{T}} > 20$ GeV;

- at least five jets with $p_{\mathrm{T}} > 55$ GeV;

- at least six jets with $p_{\mathrm{T}} > 30$ GeV. Additional jets are counted for the jet multiplicity if they satisfy $p_{\mathrm{T}} > 20$ GeV.

- at least two of the selected jets should be b-tagged by the JetFitterCombNN algorithm and have a $p_{\mathrm{T}} > 20$ GeV and $|\eta| < 2.5$;

- a transverse missing energy significance $E_{\mathrm{T}}^{\mathrm{miss}}/\sqrt{H_{\mathrm{T}}} < 3$, where H_{T} is the scalar sum of the transverse momentum of all jets in the event, to ensure the observed $E_{\mathrm{T}}^{\mathrm{miss}}$ is not due to poorly reconstructed jets;

- a minimum distance between the two b-tagged jets $\Delta R(b, \bar{b}) = 1.2$, to remove $b\bar{b}$ pairs originating from gluon splitting.

The large values for the jet p_{T} cut, 55 GeV on the fifth jet p_{T}, is due to the necessity of selecting events that are near the plateau of the multi-jet trigger efficiency turn-on curve. The lepton veto and $E_{\mathrm{T}}^{\mathrm{miss}}$ significance cuts are used to reject events from other electroweak processes. After preselection, 6114 data events are left. For the simulated signal sample, these preselection requirements give a signal efficiency of 1.1%.

4 Multi-jet QCD background modelling

The most challenging task related to the extraction of the $t\bar{t}$ production cross-section in the all-hadronic channel is the estimation of the dominant source of background: QCD multi-jet production. The strategy used in this note consists of using a data-driven procedure to reproduce the shape of the different observables from alternative data samples. This technique, labelled in the following as Event Mixing, was originally developed and successfully used in Ref.[23] to derive the $t\bar{t}$ production cross-section. The modelling of the shape of the different kinematic and topological distributions associated with the QCD multi-jet background is used to define the $t\bar{t}$ background hypothesis χ^2 template defined in Section 5. The latter is used with the signal $t\bar{t}$ template to extract the contribution of both the $t\bar{t}$ signal and the QCD multi-jet background. Other background processes included in the selected data sample are tiny by comparison. The shaping of the final χ^2 distribution by the b-tagging efficiency's dependence on jet p_{T} is taken into account since the original sample, from which the background is modelled, contains at least two b-tagged jets. These two b-tagged jets are used to mimic the b-jets coming from real top-quark decays in the signal sample.

4.1 Background modelling

The principle of the Event Mixing technique is to model a higher jet-multiplicity multi-jet sample from a lower jet-multiplicity multi-jet sample, using a similar selection but depleted of signal events. The method uses a sample with a lower number of jets (exclusive) to model a sample with a larger multiplicity: the target multiplicity is made up by adding jets to the initial sample. The technique is used to model QCD multi-jet events with at least six jets from events with a jet-multiplicity equal to exactly four or five. These four or five-jet exclusive events constitute a multi-jet sample which has a negligible amount of contamination from $t\bar{t}$ signal events. In the following, the jet numbering is based on p_{T} ordering. The algorithm proceeds as follows:

a) Three classes of events are selected: exactly four-jet events, exactly five-jet events and finally events with at least six jets. These event samples are required to have at least two b-tagged jets and no isolated lepton as defined in Section 3. Five-jet events are selected with the fifth jet $p_{\mathrm{T}} > 55$ GeV and pass the five-jet trigger. Four-jet events have to pass the four-jet trigger with a $p_{\mathrm{T}} > 80$ GeV. The inclusive six-jet events will be used as donors of low p_{T} jets. These low p_{T} jets will be added to the acceptor four-jet or five-jet events to model the inclusive six-jet QCD multi-jet background in the signal region.

b) For a given acceptor four-jet (five-jet) event, a donor event with at least six jets and similar phase space configuration is identified. This is achieved by constraining the leading jet in the four-jet (five-jet) event to match the p_{T} of the leading jet in the inclusive six-jet sample, within a $|\Delta p_{\mathrm{T}}| < 1$ GeV. Since the leading jet p_{T} is correlated with the momentum transfer of the hard scatter, this constraint ensures that the phase space for the inclusive six-jet donor event and the acceptor event with four (five) jets have similar characteristics. The common constraint on the phase space for the four-jet (five-jet) and the inclusive six-jet event is reinforced by constraining the fourth (fifth) jet in the two samples to be close in p_{T} ($|\Delta p_{\mathrm{T}}| < 1$ GeV). This additional constraint on the softest jet aims to select an event with similar characteristics on the softest donor jet.

c) In the case of a matching pair of donor and acceptor, the acceptor receives the fifth and softer jets from the donor in the case of an exclusive four-jet acceptor. In the case of an exclusive five-jet event acceptor, the sixth and softer jets from the inclusive six-jet donor are added. The four-momenta of additional jets are not modified by the algorithm. Attention is paid so that the added softer jets do

not overlap with any original jet in the four or five-jet acceptor event. This is ensured by requiring $\Delta R > 0.4$ between each pair of jets. Combinations that fail this overlap constraint are not used.

d) For each exclusive four- or five-jet acceptor event, all the inclusive six-jet events are considered for the mixing. If no matching inclusive six-jet event is found, the four or five-jet acceptor event is discarded from the list. If there are multiple matches, the acceptor event is used up to five times with different donor jets.

In the analysis, the multi-jet background with at least six jets is modelled by applying the algorithm to the exclusive five-jet QCD multi-jet data events. Since additional jets could artificially create missing transverse energy, the transverse missing energy significance requirement, as described in 3.4, is applied before the Event Mixing.

4.2 Background validation

The Event Mixing technique was shown to reproduce enriched QCD inclusive six-jet events with an independent event sample. This was done by selecting exclusive five-jet events and inclusive six-jet events triggered with the five-jet trigger signature described in Section 2 . The same procedure as described in Section 4.1 is applied, except that the events are required not to contain any b-tagged jet to guarantee to be depleted on signal events. The derived inclusive six-jet sample with no b-tagged jet was found to reproduce reasonably well the shapes of the distributions of the different observables from the inclusive six-jet QCD data without b-tagged jets. The distributions for the number of selected jets, the aplanarity[2], the centrality[3], and H_T are shown in Figure 1.

5 Cross-section measurement

To test the compatibility of selected events with the $t\bar{t}$ hypothesis by assigning jets to the different decay products and looking at the consistency of the kinematics with the expected top quark and W boson masses, a χ^2-based discriminant observable was implemented. It aims to extract the $t\bar{t}$ signal from the multi-jet background.

If there are more than two b-tagged jets, the χ^2 minimization chooses the two b-jets and the remaining b-tagged jets will not be used to reconstruct the $t\bar{t}$ system. The same principle applies in the case of more than six jets where again the χ^2 minimization chooses which six jets (including the two b-jets) will be used to form the candidate $t\bar{t}$ pairs. The χ^2 is built for each one of the six $t\bar{t}$ hypothesis. For a given event, the correct jet assignment is identified as the jet combination which minimises

$$\chi^2 = \frac{\left(m_{j_1,j_2} - m_W\right)^2}{\sigma_W^2} + \frac{\left(m_{j_1,j_2,b_1} - m_t\right)^2}{\sigma_t^2} + \frac{\left(m_{j_3,j_4} - m_W\right)^2}{\sigma_W^2} + \frac{\left(m_{j_3,j_4,b_2} - m_t\right)^2}{\sigma_t^2}, \tag{1}$$

and is used to select, among the different jets, which jets to assign to each W boson and top quark. The $t\bar{t}$ signal and the background mass χ^2 templates modelled respectively with MC@NLO and the Event Mixing technique described in the previous sections, are fitted to the χ^2 output for the selected data events. The $t\bar{t}$ signal fraction and thereby the background normalization are extracted from the likelihood fit of the χ^2 distribution. The likelihood is defined as:

$$L(f_s) = \Pi_i \frac{\mu^{n_i} \exp(-\mu_i)}{n_i!}; \;\; \mu_i = N_{\text{data}} \times (f_s \times P_{i,t\bar{t}} + (1 - f_s) \times P_{i,\text{QCD}}). \tag{2}$$

[2]The aplanarity is defined as $3\lambda_2/2$, where λ_2 is the second lowest eigenvalue of the momentum tensor $M_{\alpha,\beta} = \Sigma_i \, p_{\alpha,i} \, p_{\beta,i} / \Sigma_i \, |p_i|^2$ with i running over all jets and α, β the three spatial components of the jet four-momentum.

[3]The centrality is defined as the scalar sum of jet p_{T} divided by the invariant mass of all jets.

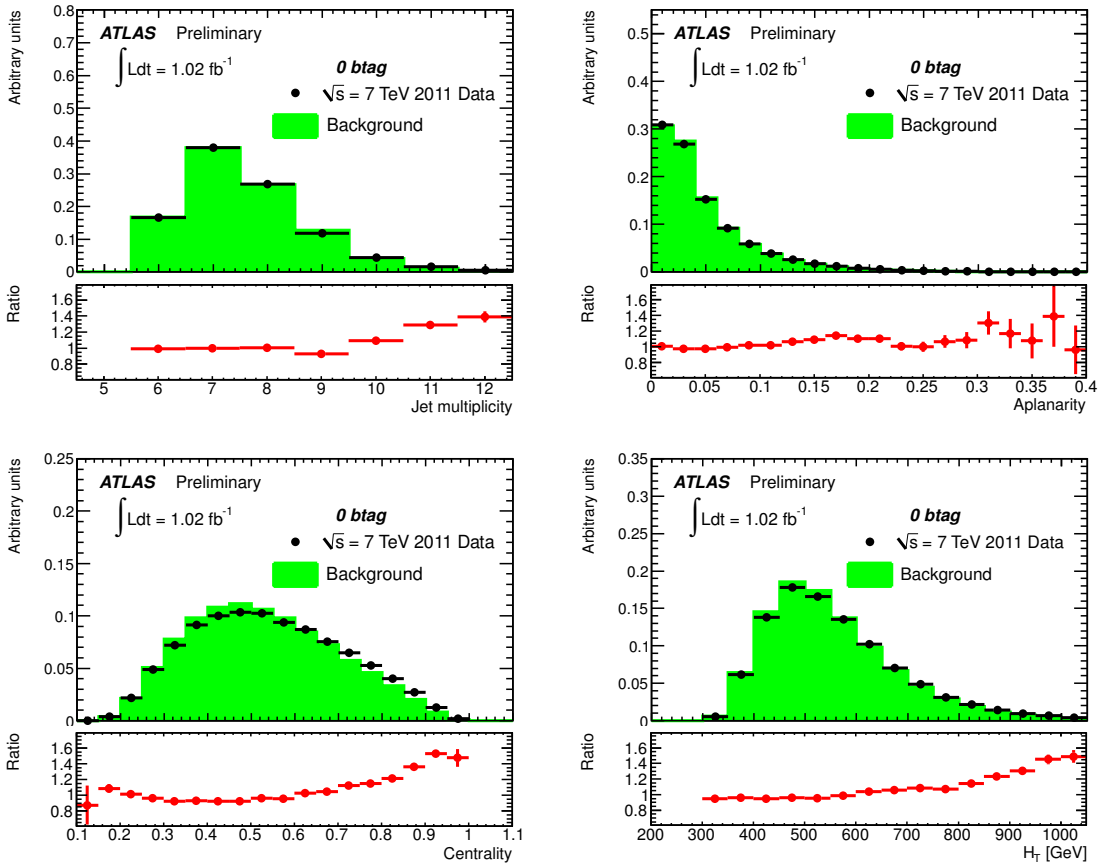

Figure 1: Comparison between inclusive six-jets data (dots) and the prediction modelled from five jet data for events without b-tagging for the number of jets, the aplanarity, the centrality and H_T. All histograms are normalized to have integral equal to one. Also shown the ratio between data and prediction.

where f_s is a parameter corresponding to the signal fraction in data and N_{data} is the number of observed data events. The symbols $P_{t\bar{t}}$ and P_{QCD} are the probabilities in the i-th χ^2 bin extracted from the $t\bar{t}$ signal and QCD multi-jet modelled background templates. The derived number of $t\bar{t}$ events is then used to estimate the $t\bar{t}$ cross-section defined as $\sigma_{t\bar{t}} = f_s N_{\text{data}}/L\epsilon$, where L is the integrated luminosity and ϵ, the signal selection efficiency in an inclusive $t\bar{t}$ sample, which includes the non all-hadronic decay modes, is estimated to be $(0.380 \pm 0.015)\%$ using the MC@NLO generator. The result of the likelihood fit is shown in Figure 2. The signal content is estimated to be $f_s = (24.0 \pm 2.4)\%$ and the total $t\bar{t}$ cross-section $\sigma = 167 \pm 18$ (stat.) pb.

Figure 3 shows the top mass distribution for the selected candidates, using the jet combinations that minimize a mass χ^2 in which the two $(m_{j,j,b} - m_t)$ terms are substituted by $(m_{j_1,j_2,b_1} - m_{j_3,j_4,b_2})$, i.e. the difference between the mass of the two three-jet triplets. This χ^2 does not make use of the top mass constraint, but only constrains the masses of the two triplets to be equal, allowing the mass that minimizes the term to be away from m_t. For the plot shown in Figure 3 the signal and background are normalized to the cross-section measured using the m_t constraint.

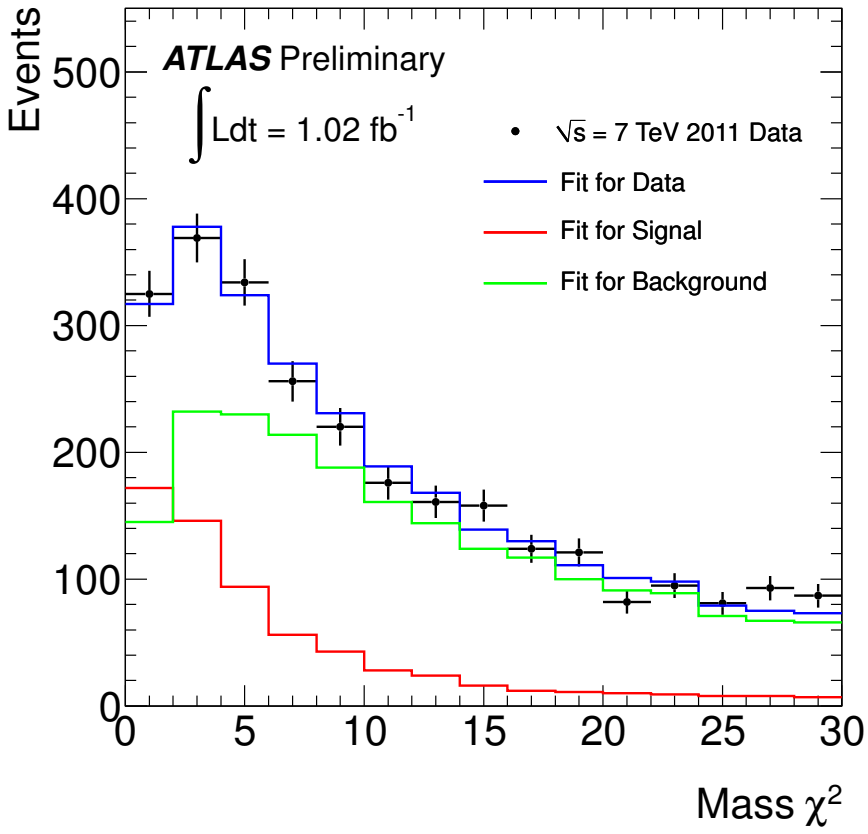

Figure 2: Fit of the minimal mass χ^2 distribution with the binned likelihood (blue line) to the selected data (dots). The $t\bar{t}$ signal fitted fraction is shown in red and the QCD inclusive six-jet background in green. The errors bars associated to the data are statistical only.

6 Cross check: the ABCD analysis

An alternative technique which relies on the definition of two uncorrelated variables to discriminate between background and signal is used. This technique, called the ABCD method, is based on counting events in control and signal regions. The background in the signal region is extracted from the yield in the control regions.

6.1 Background estimation

Two variables are used to characterize the signal: the centrality of the event and b-tagging content ϑ, which is defined as follows:

- $\vartheta = 0$ if the event contains at least one b-tagged jet.
- $\vartheta = 1$ if the event contains at least two b-tagged jets satisfying $\Delta R > 1.2$.

Four independent regions are defined: a signal enriched region `D`, and three control regions, labeled `A`, `B` and `C` dominated by multi-jet background events. Their definitions, along with the expected and the observed number of events, are given in Table 1. The signal purities and the efficiencies are given

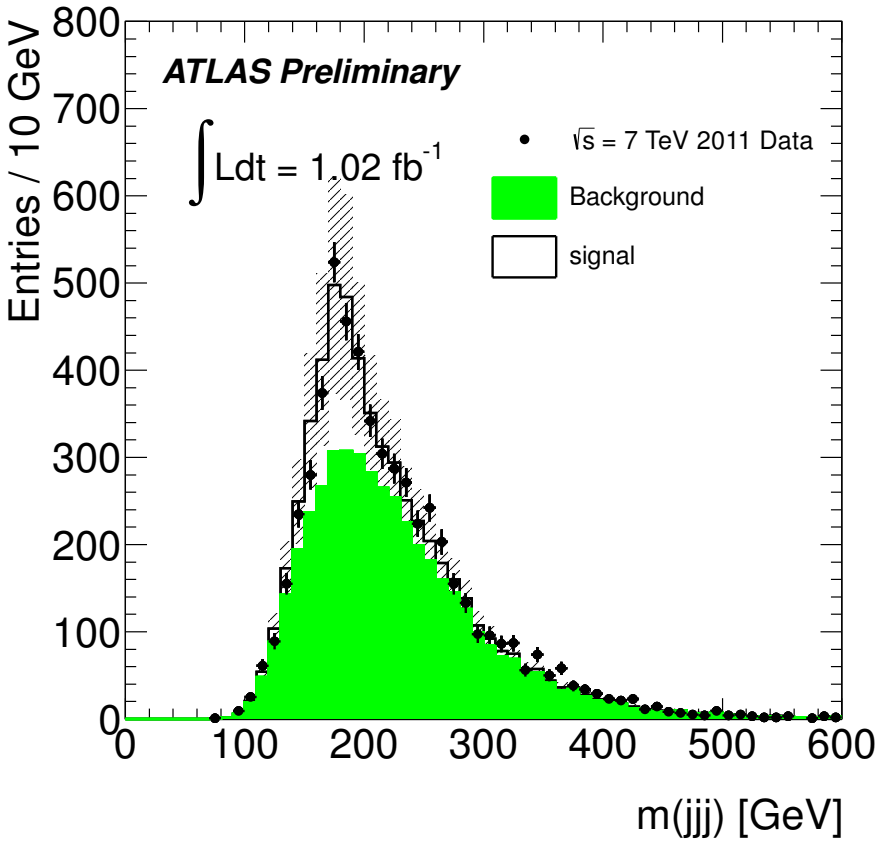

Figure 3: Top mass reconstructed from minimal mass χ^2 distribution without top-quark mass constraint, signal and background are normalized according to the result of the fit shown in Figure 2. The errors bars represent the statistical uncertainties while the hatching represent the systematic ones.

for $t\bar{t}$ events, including all decay modes. Apart from the ΔR cut and number of b-tagged jets all other pre-selection requirements described in Section 3.4 must be satisfied. Figure 4 shows the distribution of the events in the plane defined by the two variables.
The numbers of multi-jet background events in these four samples satisfy:

$$\mathrm{N}_D^{\mathrm{QCD}} \simeq \frac{\mathrm{N}_C^{\mathrm{QCD}}}{\mathrm{N}_A^{\mathrm{QCD}}} \mathrm{N}_B^{\mathrm{QCD}} \tag{3}$$

The contribution of the W+jet, Z+jet, single top and di-boson final states are estimated with Monte Carlo simulation and summarized in Table 1. Assuming a reference cross section of 164 pb for the signal, the signal fractions within the three control samples vary from 3 to 8%. The number of multi-jet background events in the selected sample can then be written as:

$$\mathrm{N}^{\mathrm{QCD}}(\sigma) = \left(\mathrm{N}_D - n_D - \epsilon_D^{t\bar{t}}\sigma L\right) = \frac{\left(\mathrm{N}_B - n_B - \epsilon_B^{t\bar{t}}\sigma L\right)\left(\mathrm{N}_C - n_C - \epsilon_C^{t\bar{t}}\sigma L\right)}{\left(\mathrm{N}_A - n_A - \epsilon_A^{t\bar{t}}\sigma L\right)} \tag{4}$$

where the acceptances $\epsilon^{t\bar{t}}$ are extracted from the simulation. They are defined using all the $t\bar{t}$ decays after the multi-jet selection.

Sample	first variable	second variable	$\epsilon^{t\bar{t}}$[%]	Signal [events]	n [events]	ρ [%]	N [events]
A	$\vartheta = 0$	Centrality < 0.65	0.57%	776	50.3	2.9%	33036
B	$\vartheta = 1$	Centrality< 0.65	0.36%	499	16.7	10.1%	6112
C	$\vartheta = 0$	Centrality > 0.65	0.49%	721	42.8	7.1%	11880
D	$\vartheta = 1$	Centrality > 0.65	0.34%	501	13.0	23.5%	2466

Table 1: Definition of the four regions, A, B, C and D. The values of n are the combined contributions of W+jet, Z+jet, single top-quark and diboson final states. The signal purities and the efficiencies are labeled ρ and $\epsilon^{t\bar{t}}$ while N is the observed number of events in each sample.

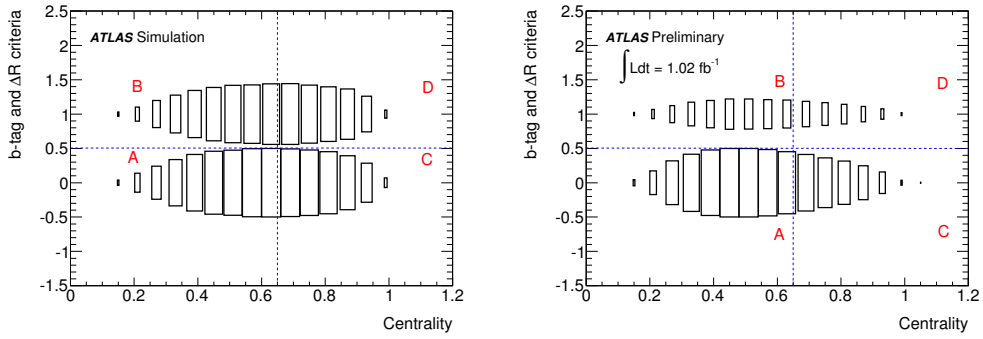

Figure 4: Distribution of simulated $t\bar{t}$ signal (left) and of data events (right) in the plane defined by the centrality and a logical variable describing the presence of at least two b-tagged jets separated by $\Delta R > 1.2$.

Since the observed N, predicted n, and expected $\epsilon^{t\bar{t}}$ are known, the second-order equation for σ can be solved:

$$\sigma = \frac{-b \pm \sqrt{\Delta}}{2a} \tag{5}$$

where $a = L^2\left(\epsilon_D^{t\bar{t}}\epsilon_A^{t\bar{t}} - \epsilon_B^{t\bar{t}}\epsilon_C^{t\bar{t}}\right)$, $b = L\left(\epsilon_B^{t\bar{t}}(\mathrm{N}_C - n_C) + \epsilon_C^{t\bar{t}}(\mathrm{N}_B - n_B) - \epsilon_D^{t\bar{t}}(\mathrm{N}_A - n_A) - \epsilon_A^{t\bar{t}}(\mathrm{N}_D - n_D)\right)$, $c = (\mathrm{N}_D - n_D)(\mathrm{N}_A - n_A) - (\mathrm{N}_B - n_B)(\mathrm{N}_C - n_C)$ and $\Delta = b^2 - 4ac$. Using the numbers of events shown in Table 1, we obtain two solutions, but only one of them is positive. The statistical uncertainties on σ are evaluated by propagating the uncertainties on N_A, N_B, N_C and N_D to the measurement. They include the statistical precision on the multi-jet background. Using the number of events given in Table 1, the signal cross-section is measured to be $\sigma = 161 \pm 38$ (stat.) pb.

7 Systematic uncertainties

Most of the systematic uncertainties are related to the signal modelling because the background is estimated by a data-driven method. The only systematic uncertainty assigned to background is the background shape modelling. For the signal $t\bar{t}$ MC sample, the systematic uncertainties are divided into shape and acceptance effects. The relative shape and acceptance uncertainties are simultaneously taken into account. The following systematic sources are considered together with an indication of whether they affect the shape or acceptance, or both:

- Jet energy scale (JES) and associated uncertainty [21], [shape and acceptance]:
  The jet energy scale and its uncertainty have been derived by combining information from test-beam data, LHC collision data and simulation. The residual differences between data and Monte

Carlo simulation have been propagated through the analysis. Additional uncertainties due to the large pile-up effects in the 2011 data are included and range from 2% to 7% as a function of the jet p_{T} and $|\eta|$. The effect of JES systematics is estimated to be 24%.

- Jet reconstruction efficiency (JRE), [shape and acceptance]:
  The difference in jet reconstruction efficiency between Monte Carlo simulation and data is propagated as a systematic uncertainty to Monte-Carlo. The effect of JRE uncertainty amounts to 0.1%.

- Jet energy resolution (JER) [24], [shape and acceptance]:
  The simulated jets are smeared to match the jet energy resolution of the data. The uncertainty due to the resolution is estimated by varying the smearing factor according to the estimated uncertainties. The effect of JER is estimated to lead to an uncertainty of 13.5%.

- Trigger efficiency, [acceptance only]:
  Events were selected with the five-jet trigger and by requiring the fifth-jet $p_{\mathrm{T}} > 55$ GeV. The associated efficiency ranges from 90% to 100%, so a conservative 10% systematic uncertainty is assigned to the trigger turn-on curve.

- LAr readout problem, [acceptance only]:
  A large fraction of the data (89.4%) used in this analysis was collected in a period during which six out of 1524 front-end boards of the liquid Argon calorimeter could not be read out. As a consequence, in the data, events with an electron or a jet pointing in the direction of this inactive region were vetoed. The same procedure is applied to the simulated events. A corresponding systematic uncertainty is evaluated by varying the jet energy threshold by ±4 GeV. The systematics on the cross-section amounts to 0.6%.

- b-tagging scale-factor (bSF) uncertainty, [shape and acceptance]:
  To take into account possible differences in b-tagging efficiency between data and MC simulations, a set of scale factors parameterised as a function of jet p_{T} and η were applied to b- , c- and light-jets. These scale factors were varied individually within their maximal associated uncertainty and propagated through the analysis. The bSF systematic uncertainty leads to a 23% uncertainty on the cross-section. This large uncertainty is due to the significant number of c-tagged jets, since the c-tagging uncertainty was conservatively assessed to be 20% (twice the b-tag scale factor uncertainty).

- Generator and parton shower (PS) dependency [shape and acceptance]:
  The uncertainty due to the modelling of the $t\bar{t}$ signal is quantified by replacing the MC@NLO Monte Carlo generator with POWHEG and PYTHIA [25] for modelling the $t\bar{t}$ signal sample. The systematic uncertainty is estimated to be 5.4%.

- Initial and Final State Radiation (ISR and FSR), [shape and acceptance]:
  The effects of variations in the amount of initial and final state radiation (ISR/FSR) were studied using the AcerMC [26] generator interfaced to PYTHIA by varying the parameters controlling ISR and FSR in a range consistent with experimental data. The systematic uncertainty is taken as half the maximum difference between any two samples. It amounts to 23%.

- Parton Distribution Function (PDF), [acceptance only]:
  The uncertainty associated to the PDF is evaluated with CTEQ6.6 and its error sets. For each of the error settings, the final cross-section is derived and the final uncertainty is calculated. The effect of PDF uncertainty amounts to 8.6%.

- Luminosity [acceptance]:
  The uncertainty on the luminosity propagates linearly to the cross-section measurement, leading to a systematic uncertainty of 3.7% [11].

- Background modelling [Event Mixing]:
  The background-modelling systematic uncertainty is estimated using a four-jet event sample. The inclusive six-jet QCD background can be modelled with the two independent exclusive samples made respectively of four-jet events and five-jet events. The effect of the difference between the QCD inclusive six-jet sample built from the exclusive four-jet sample and the one produced from the exclusive five-jet one, is included as a systematic uncertainty in the $t\bar{t}$ production cross-section. This additional modelling uncertainty, illustrated in the right-hand panel of Figure 5, is applied to the analysis based on the five-jet trigger signature bin-by-bin to the χ^2 template distribution obtained from the inclusive six-jet sample modelled from the exclusive five-jet sample. The change in the derived cross-section of 12.1% is quoted as the associated systematic uncertainty.
  An additional validation of the mixing method is performed trying it on the untagged five-jet data to predict the untagged six-jet data. The agreement on the χ^2 is shown in the left-hand panel of Figure 5.
  The dependency of the background modelling on the $|\Delta p_{\mathrm{T}}|$ constraint between the two leading jets as well as for the fifth jets is checked. The $|\Delta p_{\mathrm{T}}|$ constraint is varied from 1 GeV to 15 GeV and the maximal variation is found to be 2.3%.

- Background modelling [ABCD]:
  The estimate of the multi-jet contamination derived with the ABCD technique relies on the hypothesis that the centrality and ϑ are uncorrelated. A specific uncertainty is then associated to this measurement. Firstly, a correlation of 2% between centrality and ϑ is estimated from QCD multi-jet Monte Carlo samples. Such a correlation results in a relative uncertainty of 15% on the cross-section obtained with the ABCD method. Secondly, the centrality shape of background events was reproduced with the Event Mixing technique using four-jet and five-jet events. The shape derived from the data with this method was compared between the `B D` and `A C` regions. The shapes are verified to agree to within about 1%. The value of $\frac{\mathrm{N_{QCD}}^{C}}{\mathrm{N_{QCD}}^{A}} \times \frac{\mathrm{N_{QCD}}^{B}}{\mathrm{N_{QCD}}^{D}}$ is evaluated and found to be 1.05. This factor was introduced in Equation 5 and gives a 30% systematic effect on the cross-section. This value was taken as the systematic uncertainty due to the correlation between the centrality and ϑ.

The systematic uncertainties are summarized in Table 2 for both the event mixing and ABCD methods. Given the lower statistical and systematic uncertainties the Event Mixing is chosen to be the main result for this note.

8 Summary and conclusions

We have measured the production cross-section of top-antitop quark pairs in the all-hadronic decay channel at the LHC with a centre-of-mass energy of $\sqrt{s} = 7$ TeV and an integrated luminosity of 1.02 fb^{-1} recorded with the ATLAS detector. The shape of the dominant background, which consists of multi-jet QCD events, is modelled with a data driven technique. The cross-section is extracted with a template binned likelihood fit of the event χ^2 distribution:

$$\sigma(pp \to t\bar{t}) = 167 \pm 18 \text{ (stat.)} \pm 78 \text{ (syst.)} \pm 6 \text{ (lum.) pb}$$

which is compatible with the Standard Model expectation of $\sigma_{\mathrm{SM}} = 164^{+11}_{-16}$ pb.

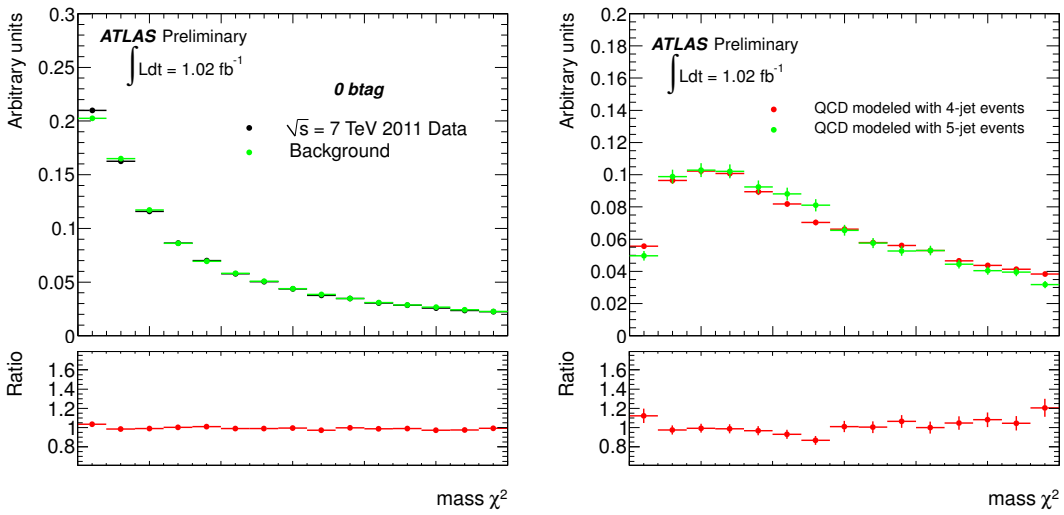

Figure 5: Left: χ^2 comparison between inclusive six-jets data (dots) and the background modelled from five-jet data (green) for events without b-tagging. Right: comparison of the two χ^2 distributions for the inclusive six-jet modelled with four-jet data (red) and the inclusive six-jet modelled with five-jet data for the four-jet trigger selected events, all events have at least two b-tagged jets. All histograms are normalized to have integral equal to one.

Source of uncertainty	Event Mixing (%)	ABCD (%)
Jet energy scale	24.2	13.7
Jet reconstruction efficiency	0.1	0.3
Jet energy resolution	13.5	6.8
Multi-jet trigger	10.0	10.0
LAr readout problem	0.6	0.3
b-tagging	23.0	30.0
Generator (PS., Hadronisation)	5.4	13.0
ISR, FSR	23.4	10.0
PDF	8.6	8.6
Luminosity	3.7	3.7
Multi-jet modelling	12.1	30.0
Total	46.7	49.9

Table 2: Summary of the different systematic uncertainties associated with the χ^2 template fit of the selected data events to the $t\bar{t}$ signal and multi-jet QCD mixed sample. Uncertainties are given in %. For the systematic uncertainties associated with the PDF, in the case of the ABCD method, the maximal variation derived from the Event Mixing based analysis is used.

References

[1] M. Aliev et al., *HATHOR: HAdronic Top and Heavy quarks crOss section calculatoR*, Comput. Phys. Commun. **182** (2011) 1034–1046, arXiv:1007.1327[hep-ph].

[2] S. Moch and P. Uwer, *Theoretical status and prospects for top-quark pair production at hadron*

colliders, Phys. Rev. **D78** (2008) 034003, arXiv:0804.1476 [hep-ph].

[3] U. Langenfeld, S. Moch, and P. Uwer, *Measuring the running top-quark mass*, Phys. Rev. **D80** (2009) 054009, arXiv:0906.5273 [hep-ph].

[4] M. Beneke, M. Czakon, P. Falgari, A. Mitov, and C. Schwinn, *Threshold expansion of the $gg(q\bar{q}) \to Q\bar{Q} + X$ cross section at $O(\alpha_s^4)$*, Phys. Lett. **B690** (2010) 483–490.

[5] K. Nakamura et al., *Particle Data Group*, J. Phys. G 37, 075021, 2010.

[6] The ATLAS Collaboration, *The ATLAS experiment at the CERN Large Hadron Collider*, JINST **3** (2008) S08003.

[7] The ATLAS Collaboration, *Measurement of the $t\bar{t}$ production cross section in the all-hadronic channel in ATLAS with $\sqrt{s} = 7$ TeV data*, ATLAS-CONF-2011-066, 2011.

[8] The ATLAS Collaboration, *Measurement of the top quark pair production cross section in pp collisions at $\sqrt{s} = 7$ TeV in dilepton final states with ATLAS*, ATLAS-CONF-2011-100, 2011.

[9] The ATLAS Collaboration, *Measurement of the top quark pair production cross section in pp collisions at $\sqrt{s} = 7$ TeV in μ+τ final states with ATLAS.*, ATLAS-CONF-2011-119, 2011.

[10] The ATLAS Collaboration, *Measurement of the $t\bar{t}$ production cross-section in pp collisions at $\sqrt{s} = 7$ TeV using kinematic information of lepton+jets events*, ATLAS-CONF-2011-121, 2011.

[11] The ATLAS Collaboration, *Luminosity Determination in pp Collisions at $\sqrt{s} = 7$ TeV using the ATLAS Detector in 2011*, ATLAS-CONF-2011-116, 2011.

[12] The ATLAS Collaboration, *ATLAS Jet Trigger in the Early $\sqrt{s} = 7$ TeV Data*, ATLAS-CONF-2010-094, 2010.

[13] S. Frixione and B.R. Webber, *Matching NLO QCD computations and parton shower simulations*, JHEP **0206** (2002) 029, hep-ph/0204244.

[14] P. M. Nadolsky et al., *Implications of CTEQ global analysis for collider observables*, Phys. Rev. **D78** (2008) 013004, arXiv:0802.0007[hep-ph].

[15] S. Frixione, P. Nason and C. Oleari, *Matching NLO QCD computations with Parton Shower simulations: the POWHEG method*, JHEP **0711** (2007) 070, arXiv:0709.2092[hep-ph].

[16] S. Agostinelli et al., *GEANT4 - A Simulation Toolkit*, Nucl. Instr. and Meth. **A506** (2003) 250.

[17] The ATLAS Collaboration, *Measurement of the top quark-pair production cross section with ATLAS in pp collisions at $\sqrt{s} = 7$ TeV*, The European Physical Journal C - Particles and Fields **71** (2011) 1–36.

[18] M. Cacciari and G. P. Salam, *Dispelling the N^3 myth for the kt jet-finder*, Physics Letters B **641** (2006) no. 1, 57 – 61.

[19] M. Cacciari, G. P. Salam, and G. Soyez, *The anti-kT jet clustering algorithm*, JHEP **04** (2008) 063, arXiv:0802.1189 [hep-ph].

[20] The ATLAS Collaboration, *Measurement of inclusive jet and dijet cross-sections in proton-proton collisions at 7 TeV centre-of-mass energy with the ATLAS detector*, Eur. Phys. J. **C 71** (2011) 1.

[21] The ATLAS Collaboration, *Update on the jet energy scale systematic uncertainty for jets produced in proton-proton collisions at $\sqrt{s}$ = 7 TeV measured with the ATLAS detector*, ATLAS-CONF-2011-007, 2011.

[22] The ATLAS Collaboration, *Commissioning of the ATLAS high-performance b-tagging algorithms in the 7 TeV collision data*, ATLAS-CONF-2011-102, 2011.

[23] The D0 Collaboration, *Measurement of the $t\bar{t}$ cross section using high-multiplicity jet events*, Phys. Rev. D **82** (2011) 032002.

[24] The ATLAS Collaboration, *Jet energy resolution and selection efficiency relative to track jets from in-situ techniques with the ATLAS Detector using Proton-Proton Collisions at a centre-of-mass energy $\sqrt{s}$ = 7 TeV*, ATLAS-CONF-2010-054, 2010.

[25] T. Sjostrand and S. Mrenna and P.Z. Skands, *PYTHIA 6.4 Physics and Manual*, JHEP **05** (2006) 026, hep-ph/0603175.

[26] B.P. Kersevan and E. Richter-Wąs, *The Monte Carlo event generator AcerMC version 2.0 with interfaces to PYTHIA 6.2 and HERWIG 6.5*, (2004) , hep-ph/0405247.